Simplified Model of CW Diffusion-Type Chemical Laser

H. MIRELS,* R. HOFLAND,† AND W. S. KING‡
The Aerospace Corporation, El Segundo, Calif.

A simplified analytical model of a diffusion-type HF chemical laser is presented. In this device, H_2 is diffused into a supersonic stream to react with F atoms and form vibrationally excited HF that is made to lase. The reaction between H_2 and F is assumed to commence at a flame sheet. A two-vibrational level model for the HF molecule is adopted. The dependence of laser amplifier and oscillator performance on diffusion rate, forward reaction rate, collisional deactivation rate, and radiative deactivation rate is determined for both laminar and turbulent diffusion.

Nomenclature

$A, \bar{A}$ = constant of order 1.0, 0.1 for laminar or turbulent diffusion, respectively
B = σ/ε
C_1, C_2, C_3 = constants, Eq. (13a)
D_1, D_2 = nondimensional parameters, Eq. (13a)
$\mathscr{D}$ = diffusion coefficient
$[F]_0$ = initial concentration of fluorine, moles/cm^3
G = net gain per semichannel, Eq. (5b)
G_0, G_m = zero power and maximum values of G, respectively
G_c = gain in oscillator cavity, Eq. (27)
g = optical gain, per unit length, Eq. (5a)
I^+, I^- = radiation intensity in $(+y)$, $(-y)$ directions, respectively
I_0, I = incident radiation, net local radiation intensity
I_s = saturation intensity, Eq. (26)
$J(\ )$ = Dawson integral, Eq. (15)
K_1, K_2 = characteristic rate parameters k_f/k_{cd}, $2BI_0/k_{cd}$
$\bar{k}$ = reaction rate, cm^3 mole^{-1} sec^{-1}, Eqs. (2) and (3)
k = product of reaction rate and concentration, sec^{-1}, Eqs. (2b) and (3b)
N_A = particles per mole
$P(x)$ = net power up to station x per semichannel, Eq. (6b)
P^*, P_e = net output power per semichannel of unit depth for amplifier or oscillator, respectively
p = static pressure, atm
p_F = partial pressure of fluorine upstream of flame sheet, atm
T = translational temperature, °K
u = axial velocity, cm/sec
w = channel semiwidth
x, x_0 = axial distance, Fig. 2
x_D = characteristic diffusion distance, $(w/A)^2u/\mathscr{D}$ or $w/\bar{A}$
y = ordinate
$y_f(x)$ = flame sheet ordinate
ε = energy (joules) per mole of photons, hvN_A
ζ = normalized axial distance, Eq. (11b)
ζ_D = diffusion parameter, Eqs. (11a) and (43)
η = ratio of laser power to value for optically saturated laser with no collisional deactivation, Eq. (10)
η_c = chemical efficiency (proportional to η)
ν = frequency
ξ, ξ_0 = alternate normalized axial distance, Eq. (13a)
σ = cross section for stimulated emission, Eq. (5a)
ϕ_i = optical cavity saturation parameter, Eq. (30b)
$[\ ]$ = moles/cm^3

Subscripts
0 = value upstream of flame sheet or value when $I = 0$
D = value at station where flame sheet reaches channel centerline
e = value at end of lasing region in oscillator
i = value at start of lasing region in oscillator
m = maximum value for amplifier

Superscripts
* = value at end of lasing region in amplifier, Eq. (18)

Presented as Paper 72-145 at the AIAA 10th Aerospace Sciences Meeting, San Diego, Calif., January 17–19, 1972; submitted February 2, 1972; revision received August 24, 1972. This work was supported jointly by the Air Force Space and Missile Systems Organization and the Air Force Weapons Laboratory of the Department of Defense under U.S. Air Force Space and Missile Systems Organization (SAMSO) Contract F04701-72-C-0073.

Index categories: Reactive Flows; Lasers.

* Head, Aerodynamics and Heat Transfer Department. Fellow AIAA.
† Member of Technical Staff. Member AIAA.
‡ Staff Scientist. Member AIAA.

Introduction

CONTINUOUS diffusion-type HF chemical lasers are currently under experimental and theoretical study. In these devices, H_2 is diffused into a supersonic jet containing atomic fluorine and a diluent (N_2 or He). The reaction between H_2 and F creates vibrationally excited HF that is made to lase in an optical cavity. In order to facilitate diffusion and geometric scaling, a multiple-grid nozzle is generally used. The diffusion-reaction regime is illustrated in Fig. 1, and experimental laser performance is described in Refs. 1–3.

The theoretical description of laser performance is quite complex and has been pursued from three different viewpoints by the present authors. First, a computer program has been developed that provides exact numerical solutions for a laser amplifier with laminar or turbulent diffusion. The flow-field

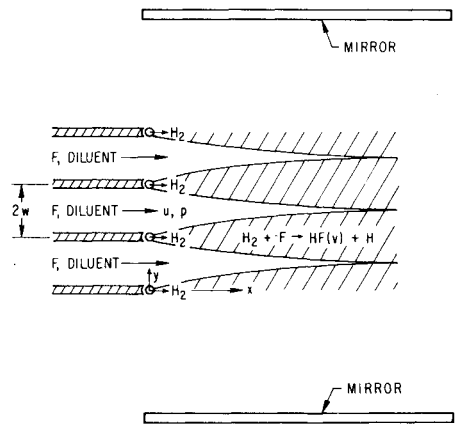

Fig. 1 Diffusion of H_2 into supersonic jet containing F atoms in chemical laser of Ref. 1.

corresponding to half of a single-nozzle exit section is considered, with a typical computation taking about 15 min. The computer program and detailed numerical results for laminar diffusion are discussed in Ref. 4. Second, an analytical laminar flame sheet solution for laser performance has been obtained.[5,6] The solution is exact in the limit where the pumping reaction is fast compared with diffusion and collisional deactivation. (These conditions are approximately satisfied in the experiments reported in Refs. 1–3.)

The third approach, which is the subject of the present paper, is to develop a simple analytic model that retains the major features of the diffusion-type chemical laser. It is assumed that laser performance depends on four characteristic rates, namely, the rate of lateral diffusion of H_2, the rate of the forward "pumping" reaction that creates vibrationally excited $HF[H_2+F \rightarrow HF(v)+H]$, the rate of collisional deactivation of vibrationally excited $HF(v)$, and the rate of radiative deactivation of $HF(v)$. The dependence of laser performance on parameters related to these rate processes, as well as on optical cavity parameters, is determined. Unlike the analyses of Refs. 4–6, the present study does not represent an exact solution; however, the results are valuable for analytically establishing scaling laws and trends for more general cases than were considered in Refs. 5 and 6.

The present model is described in the section that follows. The performance of both amplifiers and oscillators is deduced, and the resulting scaling laws are discussed. Laminar diffusion is considered in the body of the paper, and turbulent diffusion is considered in Appendix A. Although the development is in terms of an HF laser, the results are applicable to any diffusion-type chemical laser. The present paper is a condensed version of Ref. 7.

Analysis

A simplified model of a diffusion-type chemical laser is introduced in this section. The resulting equations are solved for the case of an amplifier with an incident beam of uniform intensity and for an oscillator having plane, parallel mirrors with uniform reflectivity.

A. Simplified Model

The model used herein is shown in Fig. 2. Consider a channel with half-width w and unit depth ($z = 1$). Streamlines containing atomic fluorine and a diluent are assumed to intercept a "flame sheet" defined by

$$y_f = A(\mathscr{D}x/u)^{1/2} \qquad x \leqq x_D \tag{1}$$

Symbols are defined in the Nomenclature. Equation (1) corresponds to a laminar flame sheet. The axial station x_D corresponds to the location where the flame sheet reaches the center of the channel $[x_D = (w/A)^2 u/\mathscr{D}]$. Hydrogen is introduced, generally at a stoichiometric rate, into each stream tube at the point (x_0, y) where the stream tube intercepts the flame sheet.§ The reaction between H_2 and F is assumed to commence at (x_0, y). (The latter is a departure from the usual flame sheet theory in which it is assumed that the reaction goes to completion at the flame sheet.) Lateral diffusion of reaction products across stream tubes is neglected.¶ In addition, the axial velocity u and the pressure are assumed to remain constant throughout the flowfield. Reaction exothermicity is neglected, and state properties are based on mean values of translational temperature.

A simplified two-vibrational level chemical model is adopted where HF_u and HF_l denote the lasing molecule in the upper and lower vibrational levels, respectively. The reaction between H_2 and F is assumed to produce only upper level products. Thus,

§ An alternate viewpoint is to assume that the reactants are premixed but that the reaction does not start until the flow reaches the flame sheet.

¶ The main effect of diffusion is retained in the present model by appropriate choice of the flame sheet location.

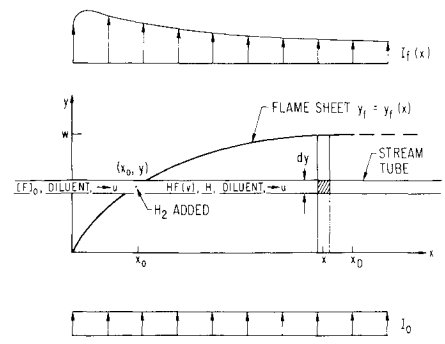

Fig. 2 Simplified model of chemical laser (amplifier case). (A single channel half-width is considered.)

$$H_2+F \xrightarrow{\bar{k}_f} HF_u+H \tag{2a}$$

and the volumetric rate of production of HF_u due to the pumping reaction may be written

$$u\frac{\partial[HF_u]}{\partial x}\bigg]_p \equiv -\frac{u\partial[F]}{\partial x} = \bar{k}_f[H_2][F]$$

$$\equiv k_f[F] \quad \text{moles/cm}^3\,\text{sec} \tag{2b}$$

The vibrationally excited HF is reduced to the lower level by molecular collisions (i.e., collisional deactivation)

$$HF_u+M \xrightarrow{\bar{k}_{cd}} HF_l+M \tag{3a}$$

$$\frac{u\partial[HF_u]}{\partial x}\bigg]_{cd} = -\bar{k}_{cd}[M][HF_u]$$

$$\equiv -k_{cd}[HF_u] \quad \text{moles/cm}^3\,\text{sec} \tag{3b}$$

or by radiative deactivation (stimulated emission less absorption)

$$\frac{u\partial[HF_u]}{\partial x}\bigg]_{rd} = -\frac{u\partial[HF_l]}{\partial x}\bigg]_{rd} = -\frac{gI}{\varepsilon} \quad \text{moles/cm}^3\,\text{sec} \tag{4}$$

where $I = I^+ + I^-$ and spontaneous emission is neglected relative to stimulated emission. The optical gain g is approximated herein by

$$g = \sigma([HF_u]-[HF_l]) \qquad \text{cm}^{-1} \tag{5a}$$

Numerical estimates for σ, which become exact in the limit $[HF_l]/[HF_u] \ll 1$, are noted in Appendix B. The net gain at each axial station (per semichannel) is

$$G(x) = \int_0^{y_f} g\,dy \tag{5b}$$

where y_f is defined by Eq. (1) for $x \leqq x_D$ and $y_f = w$ for $x > x_D$. The net radiant power per unit volume associated with the stimulated emission and absorption is

$$dP/dx\,dy\,dz = dI/dy = gI \qquad \text{w/cm}^3 \tag{6a}$$

The net power generated up to station x (per semichannel per unit channel depth) is

$$P(x) = \int_0^x dx \int_0^{y_f} gI\,dy \qquad \text{w/cm} \tag{6b}$$

Conservation of F atoms indicates

$$[F]_0 = [F]+[HF_u]+[HF_l] \qquad \text{mole/cm}^3 \tag{7}$$

where $[F]_0$ is the concentration of fluorine atoms upstream of the flame sheet. Fluorine concentration downstream of the flame sheet, for each stream tube, is found from Eq. (2b). If a mean value for k_f is assumed, the result is

$$[F]/[F]_0 = \exp[-k_f(x-x_0)/u] \qquad x \geqq x_0 \tag{8}$$

The differential equation for the distribution of HF_u along each streamline can be expressed as

$$u\{\partial[HF_u]/\partial x\} = k_f[F]-k_{cd}[HF_u]-BI([HF_u]-[HF_l]) \tag{9a}$$

where $B = \sigma/\varepsilon$. The first term on the right-hand side of Eq. (9a) represents the creation of HF_u by the pumping reaction, Eq. (2b),

while the second and third terms represent deactivation by collisions, Eq. (3b), and radiation, Eq. (4). Substitution of Eqs. (5a, 7, and 8) into Eq. (9a) yields the following expression for the variation of gain along each streamline:

$$\frac{u}{k_{cd}}\frac{\partial}{\partial x}\left(\frac{g}{\sigma[\mathrm{F}]_0}\right)+\frac{g}{\sigma[\mathrm{F}]_0}\left[1+\frac{2BI}{k_{cd}}\right]=\left(\frac{k_f}{k_{cd}}+1\right)\exp\left[-k_f(x-x_0)/u\right]-1 \qquad (9b)$$

The rates k_f and k_{cd} are assumed to be constant throughout the flowfield, and appropriate mean values are used. The solution for g is then straightforward except for the presence of I in Eq. (9b). Two cases are considered herein, namely, an amplifier and an oscillator. In each case, the variation of I with y is neglected in Eq. (9b), as will be discussed. After obtaining g from Eq. (9b), all other chemical and optical flow properties can be readily found.

Let the net laser output from an amplifier semichannel be denoted by P^*. Also, let η represent the ratio of the net laser output power P^* to the power that would be available from an optically saturated laser if there were no collisional deactivation. In the present model the latter quantity equals $\varepsilon uw[\mathrm{F}]_0/2$, because one photon is released for every two HF_u particles formed. Hence,

$$\eta = 2P^*/\varepsilon uw[\mathrm{F}]_0 \qquad (10)$$

The quantity η is a measure of the effect of collisional deactivation on laser efficiency. Accurate estimates for overall chemical laser efficiency η_c can be obtained from the expression $\eta_c = \eta_0\eta$, where η_0 is the efficiency of a saturated laser in the absence of collisional deactivation, which is evaluated in Appendix B.

Before proceeding, it is convenient to note the parameters of the present model. From Eqs. (1) and (9a), it is seen that there are four characteristic distances: x_D, u/k_f, u/k_{cd}, and $u/2BI_0$, where I_0 is a characteristic intensity. (These are the characteristic diffusion, forward pumping, collisional deactivation, and radiative deactivation distances, respectively.) The ratios of these quantities define three parameters. Suitable choices for an amplifier** are

$$K_1 = k_f/k_{cd}, \quad K_2 = 2BI_0/k_{cd}, \quad \zeta_D = x_D k_{cd}/u \qquad (11a)$$

The independent variable used herein is

$$\zeta = xk_{cd}/u \qquad (11b)$$

which is the ratio of axial distance to characteristic collisional deactivation distance. Thus, the parameters and the independent variable have been referenced to collisional deactivation.

B. Amplifier

1. *General case*

Consider a beam of uniform intensity I_0 to be incident on the reactive flow at $y = 0$ and to emerge at y_f with intensity I_f (Fig. 2). In the limit $K_2 \to \infty$ (i.e., saturated amplifier), it can be shown that $G \to 0$, $I_f/I_0 \to 1$; therefore, I can be considered everywhere constant in Eq. (9b). In the small power limit $K_2 \to 0$, the effect of radiative deactivation on g is small compared with the effect of collisional deactivation, and the solution for g is insensitive to the choice of I in Eq. (9b). It is assumed, therefore, that $I = I_0$ in Eq. (9b) for all magnitudes of I_0. The resulting solution for g is correct in the limits $K_2 \to \infty$, $K_2 \to 0$, and is approximately correct for $K_2 = 0(1)$. Within the spirit of a simplified model, I_0 can be viewed as a "characteristic value" of the lasing intensity for cases where $K_2 = 0(1)$. After $g(x, y)$ is found, the actual variation of I with x and y can readily be determined. The net power up to station x is found from $dP/dx \equiv I_f - I_0 = I_0[\exp(G)-1]$, or

$$P(x)/I_0 = \int_0^x [\exp(G)-1]\,dx \qquad (12a)$$

$$= \int_0^x G\,dx, G^2 \ll 1 \qquad (12b)$$

Integration of Eq. (9b), assuming k_f and k_{cd} are constant and $I = I_0$, yields

$$g/\sigma[\mathrm{F}]_0 = C_1\exp[-(\xi-\xi_0)] - C_2\exp[-D_1(\xi-\xi_0)] + C_3 \qquad (13a)$$

where

$$\xi = \zeta(1+K_2), \quad D_1 = K_1/(1+K_2), \quad D_2 = K_2/(1+K_2)$$
$$C_1 = D_1(2-D_2)/(D_1-1), \quad C_2 = (1+D_1-D_2)/(D_1-1),$$
$$C_3 = D_2 - 1$$

D_1 and D_2 are the ratios of k_f and $2BI_0$ to the next deactivation rate $k_{cd}+2BI_0$, respectively. Similarly, ξ is the ratio of x to the net deactivation distance $u/(k_{cd}+2BI_0)$. Equation (13a) describes the local gain downstream of the flame sheet for a streamline that enters the flame sheet at (ξ_0, y). The net gain at each axial station for an arbitrary flame sheet y_f is, from Eqs. (5b) and (13a),

$$\frac{G}{\sigma[\mathrm{F}]_0} = C_1\exp(-\xi)\int_0^{y_f}\exp(\xi_0)\,dy - C_2\exp(-D_1\xi)\int_0^{y_f}\exp(D_1\xi_0)\,dy + C_3 y_f \qquad (13b)$$

For a laminar flame sheet

$$dy = A(\mathscr{D}/u)^{1/2}dx_0^{1/2} = (w/\zeta_D^{1/2})\,d\zeta_0^{1/2}$$

and Eq. (13b) yields

$$\frac{G}{\sigma w[\mathrm{F}]_0}\left(\frac{\zeta_D}{1-D_2}\right)^{1/2} = C_1 J(\xi^{1/2}) - \frac{C_2}{D_1^{1/2}}J[(D_1\xi)^{1/2}] + C_3\xi^{1/2}, \quad \zeta \leqq \zeta_D \qquad (14a)$$

$$= C_1\exp[-(\xi-\xi_D)]J(\xi_D^{1/2}) - \frac{C_2}{D_1^{1/2}}\times \exp[-D_1(\xi-\xi_D)]J[(D_1\xi_D)^{1/2}] + C_3\xi_D^{1/2}, \quad \zeta > \zeta_D \qquad (14b)$$

where $J(\,)$ is the Dawson integral

$$J(Z) = \exp(-Z^2)\int_0^Z \exp(Z_0^2)\,dZ_0 \qquad (15a)$$

$$= Z[1-\tfrac{2}{3}Z^2+\tfrac{4}{15}Z^4+0(Z^6)] \qquad (15b)$$

$$= (2Z)^{-1}[1+(2Z^2)^{-1}+0(Z^{-4})] \qquad (15c)$$

Properties of the Dawson integral are noted in Refs. 7 and 8. The total power extracted up to station x is found from Eqs. (12) and (14). For $G^2 \ll 1$,

$$\frac{2P}{\varepsilon uw[\mathrm{F}]_0}\frac{\zeta_D^{1/2}}{D_2(1-D_2)^{1/2}} = C_1[\xi^{1/2}-J(\xi^{1/2})] - \frac{C_2}{D_1}\times\left[\xi^{1/2}-\frac{J[(D_1\xi)^{1/2}]}{D_1^{1/2}}\right] + \tfrac{2}{3}C_3\xi^{3/2}, \quad \zeta \leqq \zeta_D \qquad (16a)$$

$$= C_1[\xi_D^{1/2}-J(\xi_D^{1/2})] - \frac{C_2}{D_1}\times\{\xi_D^{1/2}-J[(D_1\xi_D)^{1/2}]\} + \tfrac{2}{3}C_3\xi_D^{3/2} + C_1\{1-\exp[-(\xi-\xi_D)]\}J(\xi_D^{1/2}) - \frac{C_2}{D_1^{3/2}}\{1-\exp[-D_1(\xi-\xi_D)]\}\times J(D_1\xi)^{1/2} + C_3\xi_D^{1/2}(\xi-\xi_D), \quad \zeta > \zeta_D \qquad (16b)$$

2. *Special cases* ($K_1 \to \infty$, $\zeta \leqq \zeta_D$)

In order to simplify the discussion of these results, we consider $K_1 \to \infty$, $\zeta \leqq \zeta_D$. The assumption $K_1 \to \infty$ implies that the pumping reaction goes to completion at the flame sheet. The assumption $\zeta \leqq \zeta_D$ implies that the flame sheet does not reach the

** For an oscillator, K_2 is replaced by ϕ_i, Eq. (30b).

center of the channel in the region of interest. With these assumptions, Eqs. (14a) and (16a) become

$$\{G/\sigma w[\mathrm{F}]_0\}[\zeta_D/(1-D_2)]^{1/2} = (2-D_2)J(\xi^{1/2})-(1-D_2)\xi^{1/2} \tag{17a}$$

$$\frac{2P}{\varepsilon uw[\mathrm{F}]_0}\frac{1}{D_2}\left(\frac{\zeta_D}{1-D_2}\right)^{1/2} = (2-D_2)[\xi^{1/2}-J(\xi^{1/2})]-\tfrac{2}{3}(1-D_2)\xi^{3/2} \qquad (G^2 \ll 1) \tag{17b}$$

Results for G are plotted vs ζ in Fig. 3, with K_2 as a parameter. The input intensity I_0 is amplified for values of ζ upstream of the station where $G = 0$. Values of P and ζ at this station are denoted by a superscript asterisk. Thus, P^* denotes the net output power from an amplifier and ζ^* denotes the streamwise length of the lasing zone. The vaue of ζ^*, as a function of K_2, is found from

$$(\xi^*)^{1/2}/J[(\xi^*)^{1/2}] = (2-D_2)/(1-D_2) \tag{18}$$

and the corresponding value of P^* is found from Eq. (17b). Values of ζ^* and laser efficiency η, obtained from Eq. (10), are tabulated in Table 1. Note that $1.13 \geqq \zeta^* \geqq 0.50$ for $0 \leqq K_2 \leqq \infty$. Thus, the length of the lasing zone is of the order of the collisional deactivation distance and is relatively insensitive to the degree of radiative saturation. The vaue of ζ at which G and $I_f - I_0$ are a maximum is denoted by subscript m and is found from

$$\xi_m{}^{1/2}J(\xi_m{}^{1/2}) = [2(2-D_2)]^{-1} \tag{19}$$

Corresponding values of ζ_m and G_m are included in Table 1.

Equations (17a) and (17b) are now examined for the limiting cases of a strong incident beam and a weak incident beam. The results are then used to deduce an expression for the effect of incident beam strength on gain.

a) Strong incident beam $[K_2 \to \infty,\ \zeta = 0(1)]$. Assume that the radiative deactivation rate is large compared with the collisional deactivation rate ($K_2 \to \infty$) and that the collisional deactivation rate is of the same order as the convective flow rate $[\zeta = 0(1)]$. This is the case where the reactive flow is optically saturated. In this limit, Eq. (17) yields

$$GK_2\zeta_D{}^{1/2}/\sigma w[F]_0 = (1/2\zeta^{1/2})[1-2\zeta][1+0(1/K_2\zeta)] \tag{20a}$$

$$2P\zeta_D{}^{1/2}/\varepsilon uw[\mathrm{F}]_0 = \zeta^{1/2}[1-\tfrac{2}{3}\zeta][1+0(1/K_2\zeta)] \qquad (G^2 \ll 1) \tag{20b}$$

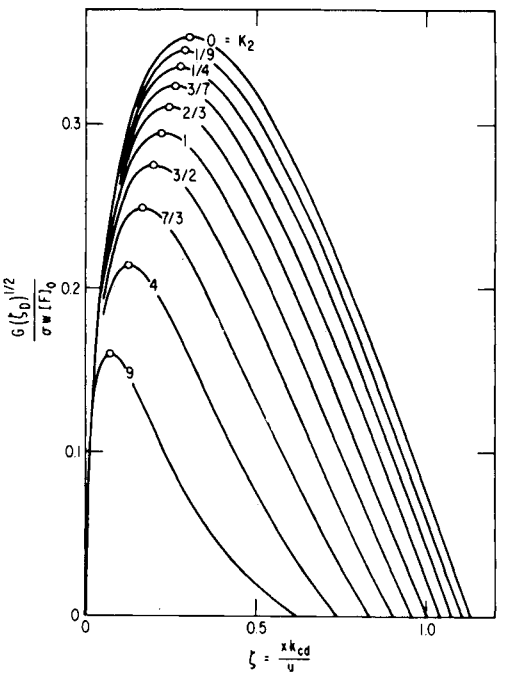

Fig. 3 Variation of integrated gain with axial distance for amplifier. $I_0 = \text{const}$, $K_1 \to \infty$, $\zeta \leqq \zeta_D$.

Table 1 Maxima for amplifier case when $I_0 = \text{const}$, $K_1 \to \infty$, Eqs. (17a) and (17b)

	Efficiency[a]		Peak gain[b]	
K_2	ζ^*	$\left(\frac{\zeta_D}{\zeta^*}\right)^{1/2}\eta$	$\frac{G_m(\zeta_D)^{1/2}}{\sigma w[\mathrm{F}]_0}$	ζ_m
0	1.1301	0.0000	0.3528	0.3051
1/9	1.1050	0.0263	0.3446	0.2926
1/4	1.0763	0.0565	0.3351	0.2788
3/7	1.0427	0.0914	0.3240	0.2629
2/3	1.0036	0.1323	0.3108	0.2438
1	0.9566	0.1811	0.2948	0.2222
3/2	0.8992	0.2403	0.2749	0.1958
7/3	0.8273	0.3140	0.2492	0.1635
4	0.7341	0.4084	0.2141	0.1237
9	0.6149	0.5310	0.1602	0.0714
∞	0.5000	0.6667	0	0

[a] For $G^2 \ll 1$, $\zeta_D \geqq \zeta^*$.
[b] For $\zeta_D \geqq \zeta_m$.

From Eq. (20a), the length of the lasing region is $\zeta^* = \frac{1}{2}$. Net output power and efficiency are

$$2P^*\zeta_D{}^{1/2}/\varepsilon uw[\mathrm{F}]_0 \equiv \eta\zeta_D{}^{1/2} = 2^{1/2}/3 \qquad \zeta_D \geqq \tfrac{1}{2} \tag{21a}$$

When $\zeta_D < \frac{1}{2}$, the optical cavity length equals ζ_D. Net output power and efficiency are then [from Eq. (20b)]

$$2P^*\zeta_D{}^{1/2}/\varepsilon uw[\mathrm{F}]_0 \equiv \eta\zeta_D{}^{1/2} = \zeta_D{}^{1/2}(1-\tfrac{2}{3}\zeta_D) \quad \zeta_D < \tfrac{1}{2} \tag{21b}$$

Equations (20a) and (20b) are not applicable near $\zeta = 0$ and, therefore, do not properly describe the behavior of ζ_m and G_m as $K_2 \to \infty$. This behavior can be deduced from Eqs. (17a) and (19). From Eq. (19) and Ref. 8, $\xi_m \to 0.8542$ as $K_2 \to \infty$, or

$$\zeta_m = 0.8542K_2{}^{-1}[1+0(K_2{}^{-1})] \tag{21c}$$

The corresponding peak gain is

$$G_m\zeta_D{}^{1/2}/\sigma w[\mathrm{F}]_0 = [1+0(K_2{}^{-1})]/2(0.8542K_2)^{1/2} \tag{21d}$$

Thus, $\zeta_m \sim K_2{}^{-1}$ and $G_m \sim K_2{}^{-1/2}$ as $K_2 \to \infty$.

b) Weak incident beam $[K_2 \to 0,\ \zeta = 0(1)]$. Assume that the radiative deactivation is small compared with the collisional deactivation ($K_2 \to 0$) and that $\zeta = 0(1)$. In this limit, Eqs. (17a) and (17b) indicate

$$G_0\xi_D{}^{1/2}/\sigma w[F]_0 = [2J(\zeta^{1/2})-\zeta^{1/2}][1+0(K_2)] \tag{22}$$

$$2P\zeta_D{}^{1/2}/\varepsilon uw[\mathrm{F}]_0 = 2K_2\zeta^{1/2}\left[1-\frac{J(\zeta^{1/2})}{\zeta^{1/2}}-\frac{\zeta}{3}\right][1+0(K_2)] \tag{23}$$

Equation (22) defines the "zero power gain," which has a maximum value of

$$(G_0)_m\zeta_D{}^{1/2}/\sigma w[\mathrm{F}]_0 = 0.3528 \tag{24}$$

at $\zeta_m = 0.305$.

If the net gain at any section is abruptly reduced to zero, the corresponding power generated at that station is $\Delta P = Gu/2B$. The power available from a diffusion-type chemical laser was estimated in Ref. 5 by reducing the zero power gain to zero at the axial station where the gain is a maximum. The present model indicates that this procedure underestimates laser efficiency by about 35% when compared with a saturated beam case. A numerically similar result is obtained in Ref. 6.

c) Saturation intensity. The present results can be used to obtain an expression relating the peak integrated gain G_m to the input intensity I_0. Equations (21d) and (24) suggest

$$G_m/(G_0)_m = [1+(I_0/I_s)]^{-1/2} \tag{25}$$

where

$$I_s = 2.351(k_{cd}/2B) \tag{26}$$

and $K_2 = 2.351I_0/I_s$. Equation (25) is exact in the limits $I_0/I_s \to 0$, $I_0/I_s \to \infty$ and is remarkably accurate for intermediate values of I_0/I_s (Fig. 4). The quantity I_s is herein termed the saturation intensity, and I_0/I_s is a measure of the reduction in peak integrated gain. Note, $G_m/(G_0)_m = 1/(2)^{1/2}$ when $I_0 = I_s$.

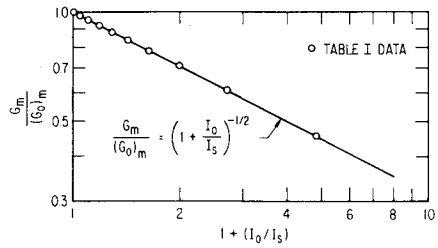

Fig. 4 Variation of peak integrated gain with amplifier input intensity, Eq. (25).

It is also seen from Table 1 that, when $I_0 = I_s$ (i.e., $K_2 = 2.35$), the output power is about half that which would be obtained from a saturated ($K_2 \to \infty$) amplifier. I_s is a state property of the optical medium and corresponds to an intensity such that the radiative deactivation rate is of the order of the collisional deactivation rate.

Equation (25) has the same form as the expression relating gain and intensity in a steady-state, uniform-optical medium that is inhomogeneously broadened.[9] This is fortuitous as the exponent $-\frac{1}{2}$ depends on the diffusion process (Appendix A).

C. Oscillator

A discussion of the performance of a diffusion-type chemical laser having a Fabry-Perot-type cavity is presented in this section.

1. *General case*

Consider a laser with n channels, each with a semiwidth w (Fig. 1). Assume that the optical cavity consists of two plane, parallel mirrors having reflectivities r_1 and r_2, respectively, which are independent of x. In the lasing region, the lasing intensity I is assumed to be constant with y and to vary with x in such a manner as to maintain the integrated gain G at the constant value[7]

$$G_c = (\ln r_1 r_2)/(-4n) \tag{27}$$

Upstream of the lasing region, the integrated gain is less than this value and the lasing intensity is zero.

Let ζ_i denote the value of ζ at which lasing commences. The radiation intensity downstream of ζ_i is found by the integration of Eq. (9b) with respect to y between the limits $y = 0$ and $y = y_f$. Solving the resulting equation for I and noting $\partial G/\partial x = 0$ in the lasing region, yields

$$\frac{2BI}{k_{cd}} = \frac{\sigma[\mathrm{F}]_0}{G_c}\left[(1+K_1)\exp(-K_1\zeta)\int_0^{y_f}\exp(K_1\zeta_0)\,dy - y_f\right] - 1 \tag{28}$$

Equation (28) is applicable for an arbitrary flame shape. For a laminar layer, Eq. (28) becomes

$$\frac{2BI}{k_{cd}} = \frac{\sigma[\mathrm{F}]_0 w}{G_c \zeta_D^{1/2}}\left[\frac{1+K_1}{K_1^{1/2}}J[(\xi K_1)^{1/2}] - \zeta^{1/2}\right] - 1 \qquad \zeta \leqq \zeta_D \tag{29a}$$

$$= \frac{\sigma[\mathrm{F}]_0 w}{G_c \zeta_D^{1/2}} \times \left[\frac{1+K_1}{K_1^{1/2}}\exp[-K_1(\zeta-\zeta_D)]J[(\zeta_D K_1)^{1/2}] - \zeta_D^{1/2}\right] - 1 \qquad \zeta > \zeta_D \tag{29b}$$

The lasing continues until $I = 0$ in Eqs. (28) or (29). The corresponding axial location is denoted by ζ_e.

2. *Special cases* ($K_1 \to \infty$, $\zeta \leqq \zeta_D$)

We now consider a laminar flame sheet in the limit $\zeta \leqq \zeta_D$ and $K_1 \to \infty$. Because $I = 0$ for $\zeta < \zeta_i$, ζ_i and G_c are related by, from Eq. (22),

$$\frac{G_c \zeta_D^{1/2}}{\sigma w[\mathrm{F}]_0} = \zeta_i^{1/2}\left[\frac{2J(\zeta_i^{1/2})}{\zeta_i^{1/2}} - 1\right] \equiv \phi_i \tag{30a}$$

From Eqs. (23), (27), and (30a),

Table 2 Parameters defining oscillator performance when gain = constant, $\zeta_e \leqq \zeta_D$, $K_1 \to \infty$, Eqs. (30–34)

ζ_i	ϕ_i	ζ_e	$\frac{B}{k_{cd}}I_i$	$\frac{P_e(\zeta_D)^{1/2}}{\varepsilon u w[\mathrm{F}]_0}$	$\left(\frac{\zeta_D}{\zeta_e}\right)^{1/2}\eta$
0.000	0.0000	0.5000	∞	0.2357	0.6667
0.002	0.0446	0.4694	124.3	0.2026	0.5914
0.004	0.0629	0.4574	61.82	0.1892	0.5596
0.006	0.0728	0.4485	41.00	0.1792	0.5350
0.008	0.0885	0.4412	30.58	0.1708	0.5142
0.010	0.0987	0.4349	24.33	0.1635	0.4958
0.012	0.1078	0.4294	20.16	0.1570	0.4793
0.014	0.1161	0.4244	17.19	0.1511	0.4640
0.016	0.1238	0.4198	14.95	0.1457	0.4498
0.018	0.1310	0.4156	13.22	0.1407	0.4366
0.020	0.1377	0.4117	11.83	0.1360	0.4240
0.022	0.1440	0.4080	10.69	0.1316	0.4122
0.024	0.1500	0.4046	9.741	0.1275	0.4009
0.026	0.1557	0.4014	8.939	0.1236	0.3901
0.028	0.1612	0.3983	8.251	0.1198	0.3797
0.030	0.1664	0.3954	7.656	0.1163	0.3698
0.040	0.1895	0.3828	5.569	0.1006	0.3252
0.060	0.2258	0.3638	3.448	0.0766	0.2539
0.080	0.2536	0.3500	2.428	0.0587	0.1983
0.100	0.2757	0.3394	1.794	0.0488	0.1538
0.120	0.2936	0.3311	1.368	0.0339	0.1177
0.140	0.3081	0.3245	1.061	0.0252	0.0884
0.160	0.3199	0.3193	0.8286	0.0182	0.0646
0.180	0.3294	0.3151	0.6449	0.0128	0.0455
0.200	0.3370	0.3118	0.4954	0.0085	0.0306
0.220	0.3428	0.3093	0.3706	0.0053	0.0191
0.240	0.3472	0.3075	0.2643	0.0029	0.0106
0.260	0.3502	0.3062	0.1720	0.0013	0.0049
0.280	0.3521	0.3054	0.0905	0.0004	0.0014
0.305	0.3528	0.3051	0.0000	0.0000	0.0000

$$\phi_i = [\zeta_D^{1/2}/\sigma w[\mathrm{F}]_0][\ln r_1 r_2/(-4n)] = 0.3528 G_c/(G_0)_m \tag{30b}$$

Thus, ϕ_i is a measure of the degree of saturation and varies in the range $0 \leqq \phi_i \leqq 0.3528$. The axial station ζ_i where lasing first begins is defined by Eq. (30). The lasing intensity downstream of ζ_i is, from Eq. (29a) with $K_1 \to \infty$,

$$2BI/k_{cd} = (1/\phi_i)[(1/2\zeta^{1/2}) - \zeta^{1/2}] - 1 \tag{31}$$

The end of the lasing zone is found by letting $I = 0$ in Eq. (31) and equals

$$\zeta_e = \tfrac{1}{4}[(\phi_i^2+2)^{1/2} - \phi_i]^2 \tag{32}$$

The variation of I with ζ is plotted in Fig. 5 for various values of ϕ_i. The value of I increases discontinuously at ζ_i from the value 0 to the value I_i, found by Eq. (31) with $\zeta = \zeta_i$. With increasing ζ, I decreases monotonically to zero at ζ_e. Corresponding values of ϕ_i, ζ_i, I_i, and ζ_e are listed in Table 2. The local power extraction per unit length is found from $dP/dx = G_c I$ or

$$\frac{2dP/dx}{\varepsilon w[\mathrm{F}]_0}\frac{\zeta_D^{1/2}}{k_{cd}} = \phi_i\frac{2BI}{k_{cd}} = \frac{1}{2\zeta^{1/2}}[1 - 2\zeta - 2\phi_i\zeta^{1/2}] \tag{33}$$

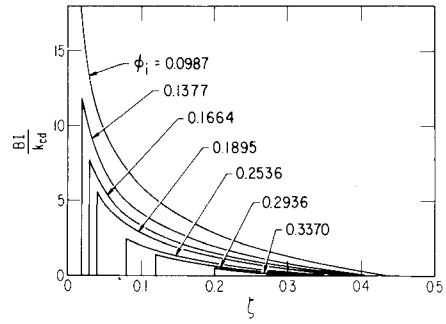

Fig. 5 Variation of lasing intensity I with ζ in oscillator cavity with constant gain, Eq. (31), $K_1 \to \infty$.

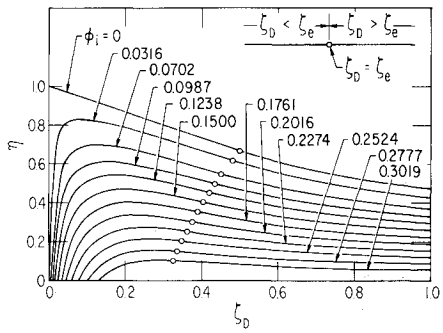

Fig. 6a Oscillator efficiency and output power, $K_1 \to \infty$, efficiency.

The total power extracted is found by the integration of Eq. (33) from ζ_i to ζ_e when $\zeta_e \leqq \zeta_D$ or from ζ_i to ζ_D when the value of ζ_e indicated by Eq. (32), is greater than ζ_D. Thus

$$\frac{2P_e\zeta_D^{1/2}}{\varepsilon uw[\mathrm{F}]_0} = \eta\zeta_D^{1/2} = \left[\zeta^{1/2} - \tfrac{2}{3}\zeta^{3/2} - \phi_i\zeta\right]_{\zeta_i}^{\zeta_e} \qquad \zeta_e \leqq \zeta_D \tag{34a}$$

$$= \left[\zeta^{1/2} - \tfrac{2}{3}\zeta^{3/2} - \phi_i\zeta\right]_{\zeta_i}^{\zeta_D} \qquad \zeta_e > \zeta_D \tag{34b}$$

Numerical results for power and efficiency are included in Table 2. Output power is reduced to zero when $\phi_i = 0.3528$. The variation of efficiency and power with ζ_D is plotted in Fig. 6. It is later shown that $(\zeta_D)^{1/2} \sim p$ for fixed w and fixed stoichiometry and initial temperature. For these conditions, Fig. 6b indicates that output power is proportional to p when $\zeta_D \to 0$ and is independent of p when $\zeta_D \gtrsim \frac{1}{2}$, as will be discussed later.

The power defined by Eq. (34) represents power extracted from the flow and includes both the power absorbed by the mirrors and the power transmitted through the mirrors.

In the limit of nearly perfectly reflecting mirrors ($\phi_i \ll 1$), the solution takes on the following form (assuming $\zeta_e \leqq \zeta_D$):

$$\zeta_i = \phi_i^2[1 + \tfrac{8}{3}\phi_i^2 + 0(\phi_i^4)] \tag{35a}$$

$$\zeta_e = \tfrac{1}{2}[1 - 2^{1/2}\phi_i + 0(\phi_i^2)] \tag{35b}$$

$$(2BI/k_{cd})\phi_i = (1/2\zeta^{1/2})[1 - 2\zeta] + 0(\phi_i) \tag{35c}$$

$$\frac{2P_e\zeta_D^{1/2}}{\varepsilon uw[\mathrm{F}]_0} = \eta\zeta_D^{1/2} = \frac{2^{1/2}}{3}\left[1 - \frac{9(2)^{1/2}}{4}\phi_i + 0(\phi_i^2)\right] \tag{35d}$$

For $\zeta_i \leqq \zeta_D \leqq \zeta_e$ and $\phi_i \to 0$, the output power and efficiency are:

$$2P_e\zeta_D^{1/2}/\varepsilon uw[\mathrm{F}]_0 = \eta\zeta_D^{1/2} = \zeta_D^{1/2}[1 - \tfrac{2}{3}\zeta_D - \phi_i\zeta_D^{1/2}] + 0(\phi_i) \tag{35e}$$

When $\phi_i \to 0$, these results are in exact agreement with the results for a saturated amplifier, Eqs. (20) and (21).

D. Instantaneous Diffusion ($\zeta_D \to 0$)

The limit $\zeta_D \to 0$ corresponds to the case where the reaction is assumed to commence at $x = 0$ for all streamlines. This occurs when 1) the diffusion rate is fast relative to the chemical rates, or 2) the reactants are premixed and the reaction is started at $x = 0$ by some perturbation of the flow (e.g., by an electrical discharge).††

The performance of an amplifier and an oscillator in the limit $\zeta_D \to 0$ is discussed in Ref. 7.

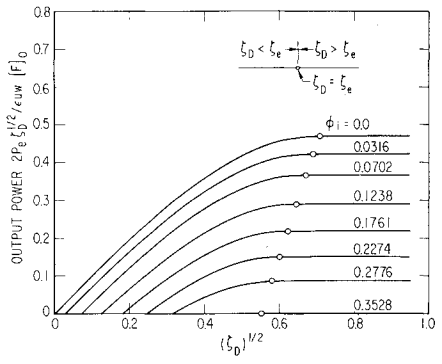

Fig. 6b Oscillator efficiency and output power, $K_1 \to \infty$, output power.

Scaling Laws for Diffusion Laser

Scaling laws are now derived, assuming laminar diffusion. (The case of turbulent diffusion is discussed in Appendix A.) The dependence of laser performance on p, u, T, and w is of particular interest.

Molecular rates are characterized herein by $\mathscr{D} \sim T^{3/2}/p$, $\bar{k}_{cd} \sim T^{\omega}$, and $\bar{k}_f \sim T^{\omega_f}$. The equation of state indicates $[\mathrm{M}] \sim p_\mathrm{M}/T$ and $[\mathrm{F}]_0 \sim p_\mathrm{F}/T$, where p_M and p_F are the partial pressures of the collisional deactivation partner M and the initial atomic fluorine concentration. When collisional deactivation is due primarily to HF – HF ($V-T$) collisions, as is generally the case, p_M can be taken equal to p_F.

As previously noted, Eqs. (11a) and (11b), diffusion laser performance is characterized by three parameters and one independent variable. The dependence of these quantities on p, u, T, and w is

$$K_1 \sim T^{\omega_f - \omega}[\mathrm{H}_2]/[\mathrm{M}] \qquad K_2 \sim [(p/p_\mathrm{M})/T^{\omega-1}][I_0/p] \sim I_0/I_s \tag{36}$$

$$\zeta_D \sim \frac{(p_\mathrm{M}/p)}{A^2T^{2.5-\omega}}p^2w^2 \qquad \zeta \sim \frac{p_\mathrm{M}/p}{T^{1-\omega}}\frac{px}{u}$$

Dependent variables in the amplifier problem are of the form

$$G\zeta_D^{1/2}/\sigma w[\mathrm{F}]_0 \sim [(T^{\omega-0.5}/\sigma^2A^2)(p_\mathrm{M}/p_\mathrm{F})(p/p_\mathrm{F})]^{1/2}G \tag{37a}$$

$$2P^*\zeta_D^{1/2}/\varepsilon uw[\mathrm{F}]_0 \sim [(T^{\omega-0.5}/A^2)(p_\mathrm{M}/p_\mathrm{F})(p/p_\mathrm{F})]^{1/2}P^*/u \tag{37b}$$

From Eqs. (14) and (16), it is seen that for amplifiers

$$G\zeta_D^{1/2}/\sigma w[\mathrm{F}]_0 = fu(K_1, K_2; \zeta) \qquad \zeta \leqq \zeta_D \tag{38a}$$

$$= fu(K_1, K_2, \zeta_D; \zeta) \qquad \zeta > \zeta_D \tag{38b}$$

$$\eta\zeta_D^{1/2} = \{2P^*\zeta_D^{1/2}/\varepsilon uw[\mathrm{F}]_0\} = fu(K_1, K_2) \qquad \zeta^* \leqq \zeta_D \tag{38c}$$

$$= fu(K_1, K_2, \zeta_D) \qquad \zeta^* > \zeta_D \tag{38d}$$

All characteristic axial lengths $\tilde{\zeta} \sim p_\mathrm{M}\tilde{x}/T^{1-\omega}u$ (such as the length of the lasing region) have the same dependence on K_1, K_2, and ζ_D as indicated in Eqs. (38c) and (38d), with ζ^* replaced by $\tilde{\zeta}$. The corresponding flame sheet ordinate is $\tilde{y}_f = w(\tilde{\zeta}/\zeta_D)^{1/2}$. In the case of an oscillator, K_2 in the preceding expressions is replaced by

$$\phi_i \sim [(T^{\omega-0.5}/\sigma^2A^2)(p_\mathrm{M}/p_\mathrm{F})(p/p_\mathrm{F})]^{1/2}[\ln r_1r_2/(-4n)] \tag{39}$$

We now examine the behavior of the dependent variables in certain limiting cases of interest. In particular, we consider a saturated medium and a nonlasing medium.

A. Saturated Amplifier ($K_2 \to \infty$) or Oscillator ($\phi_i \to 0$) in Limit $K_1 \to \infty$, $\zeta_D \geqq \frac{1}{2}$

In this case, $\zeta^* = \zeta_e = \frac{1}{2}$ and the axial length of the optical cavity x_c is

$$x_c = u/2k_{cd} \sim uT^{1-\omega}/p_\mathrm{M} \tag{40a}$$

Thus, x_c varies directly as u and inversely as p_M. The efficiency is $\eta = (2/\zeta_D)^{1/2}/3$ so that

$$\eta \sim A[T^{2.5-\omega}(p/p_\mathrm{M})]^{1/2}(pw)^{-1} \tag{40b}$$

Note that η is independent of u. If the temperature level and the molar fraction of the reactant and diluents (i.e., p_F/p) are kept constant, $\eta \sim (pw)^{-1}$. The net output power per unit flow area P^*/w is

$$P^*/w \sim A[T^{0.5-\omega}p/p_\mathrm{M}]^{1/2}(p_\mathrm{F}/p)u/w \tag{40c}$$

†† If x/u is replaced by time t, this case also corresponds to a pulsed laser wherein premixed reactants are activated at time $t = 0$ by electrical discharge or flash lamp.

Note also that P^*/w varies inversely with w and is independent of pressure level. Thus, if the flow velocity, temperature level, and the molar fractions are kept constant, the power output from a given laser configuration is then independent of pressure level.

B. Zero Power Case ($K_2 \to 0$) in Limit $K_1 \to \infty$, $\zeta_D \geqq \zeta_m$

The peak integrated gain per semichannel $(G_0)_m$ and the peak gain per unit y, $(g_0)_m$, averaged over the semichannel height have the values, from Eq. (24),

$$(g_0)_m \equiv (G_0)_m/w = 0.353\sigma[\mathrm{F}]_0/(\zeta_D)^{1/2} \sim \sigma A[T^{(1-2\omega)/4}/w][(p_\mathrm{F}/p)(p_\mathrm{F}/p_\mathrm{M})]^{1/2} \quad (41)$$

Thus, for fixed temperature levels and molar fractions, $(g_0)_m$ varies like w^{-1} and is independent of pressure level.

The dependence on p and w of the foregoing scaling laws for η, P^*/w, $(g_0)_m$, and x_c is the same as indicated in Refs. 5 and 6. The dependence on p_F/p is more complex in Refs. 5 and 6 because of a consideration of the effect of stoichiometry on the flame sheet location and the use of a more general deactivation model.

C. Numerical Example

Some typical numerical results are now noted. Reaction 2 in Table 3 appears to be the fastest deactivation rate. The expression $k_{cd}/p_\mathrm{HF} = (10^8/1.76)(400/T)^{1.27}$ agrees with Reaction 2 to within 20% for $100°\mathrm{K} \leqq T \leqq 1000°\mathrm{K}$, $v = 2$ and is used herein to characterize the deactivation. (When several deactivation rates dominate, their sum is used.) The resulting expression for ζ is

$$\zeta = 0.187 \frac{p(\mathrm{torr})x(\mathrm{cm})}{p/p_\mathrm{HF}}\left[\frac{4\times10^5}{u}\left(\frac{400}{T}\right)^{1.27}\right] \quad (42)$$

where the term in brackets is order 1 for typical devices. Laminar and turbulent expressions for ζ_D are then [using $C = 2.88\times10^{-4}$ in Eq. (B2)]

$$\left(\zeta\frac{L}{D}\right)^{1/2} = 3.27\frac{p(\mathrm{torr})w(\mathrm{cm})}{(p/p_\mathrm{HF})^{1/2}}\left[\frac{2}{A}\left(\frac{400}{T}\right)^{1.385}\right] \quad (43a)$$

$$\zeta_D{}^T = 1.87\frac{p(\mathrm{torr})w(\mathrm{cm})}{p/p_\mathrm{HF}}\left[\frac{0.1}{\bar{A}}\left(\frac{4\times10^5}{u}\right)\left(\frac{400}{T}\right)^{1.27}\right] \quad (43b)$$

When $K_1 \to \infty$, $K_2 \to \infty$, laser output power remains constant for values of ζ_D above $\zeta_D{}^L = \frac{1}{2}$, $\zeta_D{}^T = 1$. The corresponding (critical) values of pw are

$$\left[p(\mathrm{torr})w(\mathrm{cm})\right]_{CR}^{L} = 0.217\left(\frac{p}{p_\mathrm{HF}}\right)^{1/2}\left[\frac{A}{2}\left(\frac{T}{400}\right)^{1.385}\right] \quad (44a)$$

$$\left[p(\mathrm{torr})w(\mathrm{cm})\right]_{CR}^{T} = 0.535\frac{p}{p_\mathrm{HF}}\left[\frac{0.1}{\bar{A}}\frac{u}{4\times10^5}\left(\frac{T}{400}\right)^{1.27}\right] \quad (44b)$$

For $w = 0.2$ cm, $p/p_\mathrm{HF} = 10$ and, taking the bracketed terms to be one in Eqs. (44), the critical pressures are approximately 3 and 26 torr for laminar and turbulent flow, respectively. The output power will remain constant with increases in pressure above these critical values.

Concluding Remarks

The present model describes the dependence of laser performance on the major rate processes in a diffusion-type chemical laser. The predicted effect of pressure level and laser geometry on laser efficiency, power, cavity length, and peak gain is in good agreement with the exact calculations for an HF laser amplifier presented in Ref. 4. The effects of variations in p_F/p deduced in Ref. 4 are not modeled as accurately.

In view of the many simplifications introduced, the numerical results should be viewed as qualitative rather than quantitative. Improvements can be made in the vibrational model used herein; however, the added complexity may be questionable in view of the simplified diffusion model, the lack of consideration of the energy equation, and the use of mean rates. The present model compensates for the lack of an accurate vibrational model for an HF laser by basing the computation of gain and chemical efficiency on the departure from accurate no-collisional deactivation estimates of these quantities, as discussed in Appendix B.

Appendix A: Turbulent Diffusion

The present development can be applied to arbitrary flame sheet shapes. Laminar diffusion is considered in the body of the report, and turbulent diffusion is considered in this Appendix. It is assumed that $y_f = \bar{A}x$ for $x \leqq x_D$, where $x_D = w/\bar{A}$ and $\bar{A}$ is a constant of order 0.1 (e.g., Ref. 10). The mathematical development parallels the laminar case.

A. Amplifier

It is found from Eq. (13b) that

$$(G/\sigma w[\mathrm{F}]_0)[\zeta_D/(1-D_2)] = C_1(1-e^{-\xi}) - (C_2/D_1)(1-e^{-D_1\xi}) + C_3\xi \qquad \xi \leqq \xi_D \quad (A1a)$$

$$= C_1 e^{-\xi}(e^{\xi_D}-1) - (C_2/D_1)\times e^{-D_1\xi}(e^{D_1\xi_D}-1) + C_3\xi_D \qquad \xi > \xi_D \quad (A1b)$$

The total power extracted up to station x is (for $G^2 \ll 1$)

$$\frac{2P}{\varepsilon uw[\mathrm{F}]_0}\frac{\zeta_D}{D_2(1-D_2)} = \left\{C_1(\xi_0+e^{-\xi_0}) - \frac{C_2}{D_1}\left(\xi_0 + \frac{e^{-D_1\xi_0}}{D_1}\right) + \frac{C_3}{2}\xi_0{}^2\right\}_{\xi_0=0}^{\xi_0=\xi} \qquad \xi \leqq \xi_D \quad (A2a)$$

$$\frac{2P}{\varepsilon uw[\mathrm{F}]_0}\frac{\zeta_D}{D_2(1-D_2)} = \left\{\right\}_{\xi_0=0}^{\xi_0=\xi_D} + \left[C_1(1-e^{\xi_D})\,e^{-\xi_0} + \frac{C_2}{D_1{}^2}(e^{D_1\xi_D}-1)\,e^{-D_1\xi_0} + C_3\xi_D\xi_0\right]_{\xi_0=\xi_D}^{\xi_0=\xi} \qquad \xi > \xi_D \quad (A2b)$$

1. *Special case* ($K_1 \to \infty$, $\zeta \leqq \zeta_D$)

In the limit $K_1 \to \infty$, $\zeta \leqq \zeta_D$, Eqs. (A1a) and (A2a) become

$$(G/\sigma w[\mathrm{F}]_0)\zeta_D/(1-D_2) = (2-D_2)(1-e^{-\xi}) + C_3\xi \quad (A3a)$$

$$(2P/\varepsilon uw[\mathrm{F}]_0)\zeta_D/D_2(1-D_2) = (2-D_2)(\xi+e^{-\xi}-1) + (C_3/2)\xi^2 \quad (A3b)$$

The peak value of G occurs at $\xi_m = \ln(2+K_2)$ and has the value

$$(G_m/\sigma w[\mathrm{F}]_0)\zeta_D = [1/(1+K_2)]\{1-[\ln(2+K_2)/(1+K_2)]\} \quad (A4)$$

It follows that

$$G_m/(G_m)_0 = [1+K_2-\ln(2+K_2)]/[(1-\ln 2)(1+K_2)^2] \quad (A5)$$

This expression can be approximated by

$$G_m/(G_m)_0 \doteq [1+I_0/I_s]^{-1} \quad (A5a)$$

where $I_s = 3.259I_0/K_2$. Note the difference from the laminar case, Eq. (26). The maximum output power P^* is found by substituting the value of ξ^*, defined by

$$(2-D_2)(1-e^{-\xi^*}) + C_3\xi^* = 0 \quad (A6)$$

in Eq. (A3b).

2. *Special case* ($K_1 \to \infty$, $K_2 \to \infty$)

In the limit $K_1 \to \infty$, $K_2 \to \infty$, $K_1/K_2 \to \infty$, the length of the positive gain region is

$$\zeta^* = 1 \qquad \zeta_D \geqq 1 \quad (A7a)$$

$$= \zeta_D \qquad \zeta_D \leqq 1 \quad (A7b)$$

and amplifier efficiency is given by

$$\eta\zeta_D = 1/2 \qquad \zeta_D \geqq 1 \quad (A8a)$$

$$= \zeta_D[1-(\zeta_D/2)] \qquad \zeta_D \leqq 1 \quad (A8b)$$

Table 3 Reaction rates and characteristic times for HF laser

a) Reaction rates[11]

Reaction No.	Reaction (ΔH = Kcal/mole)	Rate ($\bar{k}$, cc/mole-sec)
1	$F+H_2 \rightarrow HF(v)+H \quad v=0,1,2,3$	$15.9\times10^{13}\times10^{-350/T}$
1a	$F+H_2(0) \rightarrow HF(0)+H+31.7$	$1.2\times10^{13}\times10^{-350/T}$
1b	$F+H_2(0) \rightarrow HF(1)+H+20.4$	$2.4\times10^{13}\times10^{-350/T}$
1c	$F+H_2(0) \rightarrow HF(2)+H+9.6$	$8.2\times10^{13}\times10^{-350/T}$
1d	$F+H_2(0) \rightarrow HF(3)+H-0.8$	$4.1\times10^{13}\times10^{-350/T}$
2	$HF(v)+HF \rightarrow HF(v-1)+HF$	$v(10^{4.37}T^{2.3}+10^{13}T^{-0.4})$
3	$HF(v)+H_2 \rightarrow HF(v-1)+H_2$	$v(5\times10^5\times T^{2.08})$

b) Characteristic times ($p\tau \equiv p/k$ = atm − sec)

Reaction No.	T, °K	100	200	300	400	500	600	700	800	900	1000
1	$(p_{H_2}/k_f)\times10^9$	162.2	5.79	2.27	1.55	1.29	1.19	1.14	1.13	1.14	1.15
2(v=2)	$(p_{HF}/k_{cd})\times10^8$	0.259	0.681	1.19	1.76	2.36	2.96	3.55	4.10	4.59	5.02
3(v=2)	$(p_{H_2}/k_{cd})\times10^8$	56.8	26.9	17.3	12.7	9.98	8.20	6.94	6.01	5.29	4.72

B. Oscillator

The lasing intensity downstream of ζ_i is, from Eq. (29),

$$\frac{2BI}{k_{cd}} = \frac{1}{\phi_i}\left\{\frac{1+K_1}{K_1}\, e^{-K_1(\zeta-\zeta_0)} - \zeta_0\right\}_{\zeta_0=0}^{\zeta_0=\zeta} - 1, \qquad \zeta \leqq \zeta_D \quad \text{(A9)}$$

where $\phi_i = \zeta_D G_c/\sigma w[F]_0$. The upper limit is replaced by $\zeta_0 = \zeta_D$ for $\zeta \geqq \zeta_D$.

1. Special case ($K_1 \rightarrow \infty, \zeta \leqq \zeta_D$)

In the limit $K_1 \rightarrow \infty, \zeta \leqq \zeta_D$, Eq. (A9) reduces to

$$2BI/k_{cd} = \phi_i^{-1}(1-\zeta)-1 \quad \text{(A10)}$$

The lasing initiates the ends at ζ_i and ζ_e, respectively, which are obtained from

$$2(1-e^{-\zeta_i})-\zeta_i = \phi_i \quad \text{(A11)}$$

$$\zeta_e = 1-\phi_i \quad \text{(A12)}$$

The net output power and efficiency are

$$\frac{2P_e\zeta_D}{\varepsilon u w[F]_0} = \eta\zeta_D = \left(\zeta - \frac{\zeta^2}{2} - \phi_i\zeta\right)_{\zeta=\zeta_i}^{\zeta=\zeta_e} \quad \text{(A13)}$$

which reduces to Eq. (A8b) when $\phi_i = \zeta_i = 0$. When $\zeta_D < 1-\phi_i$, ζ_e is replaced by ζ_D.

C. Scaling Laws

The present results indicate that for turbulent diffusion

$$G\zeta_D/\sigma w[F]_0 = fu(K_1, K_2; \zeta) \qquad \zeta \leqq \zeta_D \quad \text{(A14a)}$$

$$= fu(K_1, K_2, \zeta_D; \zeta) \qquad \zeta > \zeta_D \quad \text{(A14b)}$$

$$\eta\zeta_D = fu(K_1, K_2) \qquad \zeta^* \leqq \zeta_D \quad \text{(A14c)}$$

$$= fu(K_1, K_2, \zeta_D) \qquad \zeta^* > \zeta_D \quad \text{(A14d)}$$

where $\zeta_D \sim wp_M/(\bar{A}uT^{1-\omega})$. When K_1 and K_2 are held constant and $\zeta \leqq \zeta_D$, it is found that

$$G_m \sim \sigma\bar{A}(u/T^\omega)(p_F/p_M) \quad \text{(A15a)}$$

$$\eta \sim \bar{A}(uT^{1-\omega})/(p_M w) \quad \text{(A15b)}$$

$$x^* \sim uT^{1-\omega}/p_M \quad \text{(A15c)}$$

The results for G_m and η differ from the corresponding laminar expressions, Eqs. (40b) and (41). If $p_M = p_F$, G_m is independent of pressure level p and fluorine mole fraction p_F/p. Also, G_m and η are proportional to u. The latter results would be modified if $\bar{A}$ is a function of the flow variables.

Appendix B: HF Laser Performance Considerations

Processes affecting the performance of an HF laser (employing atomic fluorine) are considered in this Appendix. In particular, forward reaction rates, collisional deactivation rates, diffusion rates, optical gain, and chemical efficiency are discussed.

A. Forward Reaction

The over-all forward reaction rate is given by Reaction 1 in Table 3. The characteristic time to consume F atoms ($\tau \equiv k_f^{-1} = 82.06T/\bar{k}_f p_{H_2}$) is also tabulated as a function of temperature. The rates at which each individual vibrational level is populated are given by Reactions 1a to 1d. The latter define the relative population in each vibrational level prior to deactivation

$$z_0 : z_1 : z_2 : z_3 = 0.075 : 0.151 : 0.516 : 0.258 \quad \text{(B1)}$$

B. Collisional Deactivation

A variety of V–T and V–V deactivation rates are noted in Ref. 11. The fastest rates appear to be V–T collisions between HF(v) and HF or H_2. The latter rates, as well as characteristic times, are included in Table 3.

C. Laminar Diffusion

The laminar diffusion coefficient can be approximated by

$$\mathscr{D} = CT^{3/2}/p \qquad \text{cm}^2/\text{sec} \quad \text{(B2)}$$

where $C = 1.56\times10^{-4}$, 2.88×10^{-4} for H_2 diffusing into N_2 or He (diluent) streams, respectively.

D. Gain

Consider diatomic molecules. Assume that the molecules in each vibrational level v are in rotational equilibrium and let $\alpha \equiv \theta_R/T_R$, where θ_R is the rotational "characteristic" temperature and T_R is the rotational temperature (taken equal to T). Denote rotational energy quantum numbers by J. The gain associated with a P-branch transition from the state $(v+1, J-1)$ to the state (v, J) is denoted by $g_{v,J}$ and may be expressed (for inhomogeneously broadened lines)[12]

$$\frac{g_{v,J}}{K|M_{v,J}|^2(W/T)^{1/2}} = \frac{\alpha J \exp[-\alpha J(J-1)]}{[1+0(\alpha)]}\left[n_{v+1} - n_v \exp(-2\alpha J)\right] \quad \text{(B3)}$$

where $K = 3.95\times10^{47}$ (°K/g-mole)$^{1/2}$/erg-cm, $|M_{v,J}|^2$ is the electric dipole moment, W is the molecular weight, and n_v is the concentration (moles/cm^3) of particles in level v. The value of J for which $g_{v,J}$ is a maximum is

$$J = (2\alpha)^{-1/2}[1+0(\alpha^{1/2})] \quad \text{(B4a)}$$

and the corresponding value of $g_{v,J}$ is

$$[(g_{v,J})_{\max}/K|M_{v,J}|^2(W/T)^{1/2}] = (\alpha/2e)^{1/2} \times \{n_{v+1} - n_v \exp[-(2\alpha)^{1/2}]\}[1+0(\alpha^{1/2})] \quad \text{(B4b)}$$

For HF, $W = 20$, $\theta_R = 29.6(1-0.037v)$°K, and $|M_{v,J}|^2 = (1.2\pm0.2)(v+1)\cdot 10^{-38}$ erg cm^3 in the range $0 \leqq v \leqq 2$, $1 \leqq J \leqq 7$.

A suitable estimate for the quantity σ, introduced in Eq. (5a), can be obtained from the relation $\sigma_{v,J} \equiv g_{v,J}/n$, where the ratios $n_v/n = z_v$, $n_{v+1}/n = z_{v+1}$, needed to evaluate $g_{v,J}$, are obtained from Eq. (B1). Equation (5a) is then exact when there is no deactivation (i.e., $[HF_l] = 0$), and is approximately correct when $[HF_l] \neq 0$. Peak values of σ for the HF laser, obtained from Eq. (B4b), are then

$$T\sigma_{1,J} = 3.3\times 10^{10}[1+0(\alpha^{1/2})] \quad \text{°K cm}^2\text{/mole} \quad \text{(B5a)}$$

$$T\sigma_{0,J} = 3.5\times 10^{9}[1+0(\alpha^{1/2})] \quad \text{°K cm}^2\text{/mole} \quad \text{(B5b)}$$

where the corresponding value of J is found by Eq. (B4a). Equation (B5b) neglects cascading effects (i.e., pumping of 1–0 transition by 2–1 transition).

E. Chemical Efficiency

Chemical efficiency η_c is defined as the ratio of laser output power to the power available from the chemical pumping reaction (i.e., 31.7 kcal/mole of atomic fluorine flow/sec). This efficiency can be analytically estimated in two steps. First, the efficiency of an optically saturated laser in the absence of collisional deactivation, denoted by η_0, can be estimated. This efficiency is associated with the relative rates at which each vibrational level is pumped. Then, the ratio of laser output with collisional deactivation to the value of saturated laser output without collisional deactivation can be estimated. (The latter, termed η, is evaluated in the body of the report.) The over-all chemical efficiency is then $\eta_c = \eta_0\eta$. A technique for determining η_0 is described in Refs. 5 and 6. The positive optical gain associated with the pumping reaction is reduced to zero for all P-branch transitions, and the corresponding output power is determined. By use of the relative pumping rates of Eq. (B1), it is found that $0.17 \leqq \eta_0 \leqq 0.21$ for $0.01 \leqq \alpha \leqq 0.10$.

References

[1] Spencer, D. J., Mirels, H., and Durran, D. A., "Performance of cw HF Chemical Laser with N_2 or He Diluent," *Journal of Applied Physics*, Vol. 43, No. 3, March 1972, pp. 1151–1157.

[2] Spencer, D. J., Mirels, H., and Jacobs, T. A., "Initial Performance of a CW Chemical Laser," *Opto-Electronics*, Vol. 2, No. 3, Aug. 1970, pp. 155–160.

[3] Mirels, H. and Spencer, D. J., "Power and Efficiency of a Continuous HF Laser," *IEEE Journal of Quantum Electronics*, Vol. QE-7, No. 11, Nov. 1971, pp. 501–507.

[4] King, W. S. and Mirels, H., "Numerical Study of a Diffusion-Type Chemical Laser," *AIAA Journal*, Vol. 10, No. 12, Dec. 1972, pp. 1647–1654.

[5] Hofland, R. and Mirels, H., "Flame Sheet Analysis of CW Diffusion-Type Chemical Laser, I. Uncoupled Radiation," *AIAA Journal*, Vol. 10, No. 4, April 1972, pp. 420–428.

[6] Hofland, R. and Mirels, H., "Flame Sheet Analysis of CW Diffusion-Type Chemical Laser, II. Coupled Radiation," *AIAA Journal*, Vol. 10, No. 10, Oct. 1972, pp. 1271–1280.

[7] Mirels, H., Hofland, R., and King, W. S., "Simplified Model of CW Diffusion-Type Laser," AIAA Paper 72-145, San Diego, Calif., 1972.

[8] Abramowitz, M. and Stegun, I. A., *Handbook of Mathematical Functions*, National Bureau of Standards, AMS 55, June 1964, p. 319.

[9] Maitland, A. and Dunn, M. H., *Laser Physics*, Wiley, New York, 1969, p. 181.

[10] Schlichting, H., *Boundary Layer Theory*, 4th ed., McGraw-Hill, New York, 1960, p. 599.

[11] Cohen, N., "A Review of Rate Coefficients for Reactions in the H_2–F_2 Laser System," TR-0172(2779)-2, Sept. 1971, The Aerospace Corp., El Segundo, Calif.

[12] Patel, C. K. N., "Continuous-Wave Laser Action in Vibrational-Rotational Transitions of CO_2," *Physical Review*, Vol. 136, No. 5A, Nov. 1964, pp. A1187–A1193.